Supramolecular rectangles through directional chalcogen bonding

Arun Dhaka, Olivier Jeannin, Emmanuel Aubert, Enrique Espinosa and Marc Fourmigué

Supplementary information

Content

A. Synthetic procedures

General considerations: Oxygen- and moisture-sensitive experiments were carried out under a dry oxygen-free nitrogen atmosphere using standard Schlenk techniques. Solvents were dried by standard methods. The NMR spectra were recorded on Bruker spectrometers (300 MHz) referenced to residual solvent signals as internal standards. Elemental analyses were performed at BioCIS (Elementar Vario/Perkin Elmer 2400 series). Commercially available compounds 1,8-Dichloroanthraquinone , 1,2-bis(4-pyridyl)ethane (bpe), 4,4'-azopyridine (azopy) were purchased and used as received. 1,4-Di(4-pyridyl)piperazine (bipy-pip) was prepared as previously described.[1] Me_2Te_2 was preliminary prepared and stored at −20 °C in an argon flushed round bottom flask according to literature.[2]

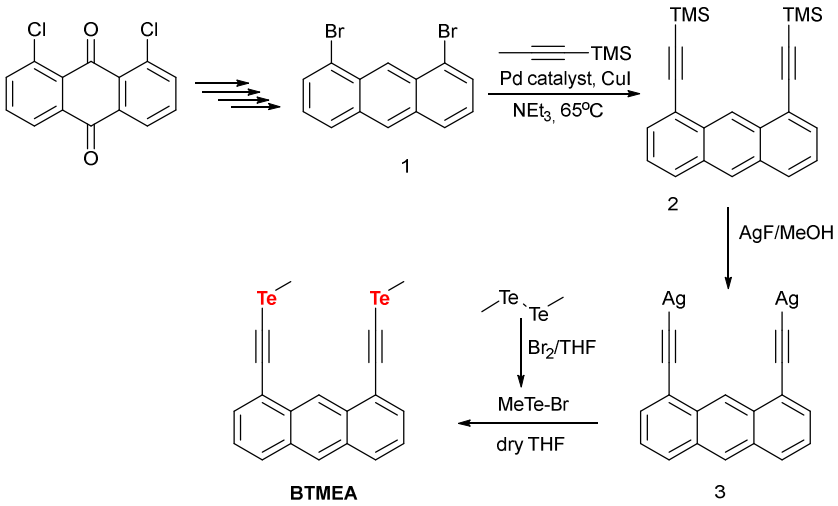

1,8-Dibromoanthracene (**1**) – This compound was synthesized from 1,8-dichloroanthraquinone in four steps using known methods in literature.[3]

1,8-Bis((trimethylsilyl)ethynyl)anthracene (2) – 1,8-Dibromoanthracene was (770 mg, 2.3 mmol) was placed in an oven dried 100 ml round bottom flask. Anhydrous trimethylamine (50 ml) was added under argon followed by TMS-acetylene (0.81 ml, 5.72 mmol, 2.5 eq). $PdCl_2(PPh_3)_2$ (162 mg, 0.23 mmol, 0.1 eq.) and CuI (43mg, 0.23 mmol, 0.1 eq.) were then added to the reaction mixture under argon and the mixture was refluxed overnight. The reaction mixture was cooled down to room temperature and the precipitate formed was filtered off. Trimethylamine was evaporated using rotary evaporator under reduced pressure and the crude solid residue was subjected to flash column chromatography on silica gel for purification (eluent: petroleum ether/ethyl acetate) to afford **2** (640 mg, 73%) as a yellow-green solid. R_f = 0.5 (petroleum ether/ethyl acetate 1 : 0.1); ^{1}H NMR (300 MHz, $CDCl_3$): δ 9.35 (s, 1H), 8.44 (s, 1H), 8.01 (d, *J* = 8.5 Hz, 2H), 7.81 (dd, *J* = 6.9, 1.1 Hz, 2H), 7.44 (dd, *J* = 8.5, 6.9 Hz, 2H), 0.41 (s, 18H).[4]

1,8-Bis(telluromethylethynyl)anthracene (BTMEA) : Compound **2** (200 mg, 0.54 mmol) was dissolved in dry methanol (25 ml) and a suspension of AgF (144 mg, 1.13 mmol, 2.1 eq.) in methanol (15 ml) was added, giving an immediate precipitate of the silver acetylide **3**. ***CAUTION. Silver acetylides are known to be explosive and should be handled with care, avoiding grinding.*** Reaction was continued for another 2h and solvent was evaporated using rotary evaporator under reduced pressure. The obtained yellow solid was dried under vacuum and suspended in dry THF (25 ml).

Besides, Me_2Te_2 (154 mg, 0.54 mmol) was dissolved in dry THF (10 ml) and treated with Br_2 (1M solution in dry CH_2Cl_2, 0.54 ml, 0.54 mmol, 1eq.) at 0°C, resulting in the formation of MeTeBr. This dark red solution was brought to room temperature and added to the silver acetylide **3** suspension. The reaction mixture was stirred for 2h. The precipitate was filtered through a Celite® pad and the filtrate was concentrated using rotary evaporator. The crude product (55mg, 20%) was pure enough to use directly off the flask as red solid, R_f = 0.35 (petroleum ether/ethyl acetate, 1 : 0.2). Mp: 142 °C. ^{1}H NMR (300 MHz, $CDCl_3$): δ 9.35 (s, 1H), 8.44 (s, 1H), 8.01 (d, *J* = 8.5 Hz, 2H), 7.81 (dd, *J* = 6.9, 1.1 Hz, 2H), 7.44 (dd, *J* = 8.5, 6.9 Hz, 2H), 5.33 (DCM) 0.41 (s, 18H). ^{13}C NMR (300 MHz, $CDCl_3$): 131.8, 131.4, 130.8, 129, 127.4, 125, 124 .1, 121.8, 109, 50.2, -13.75.

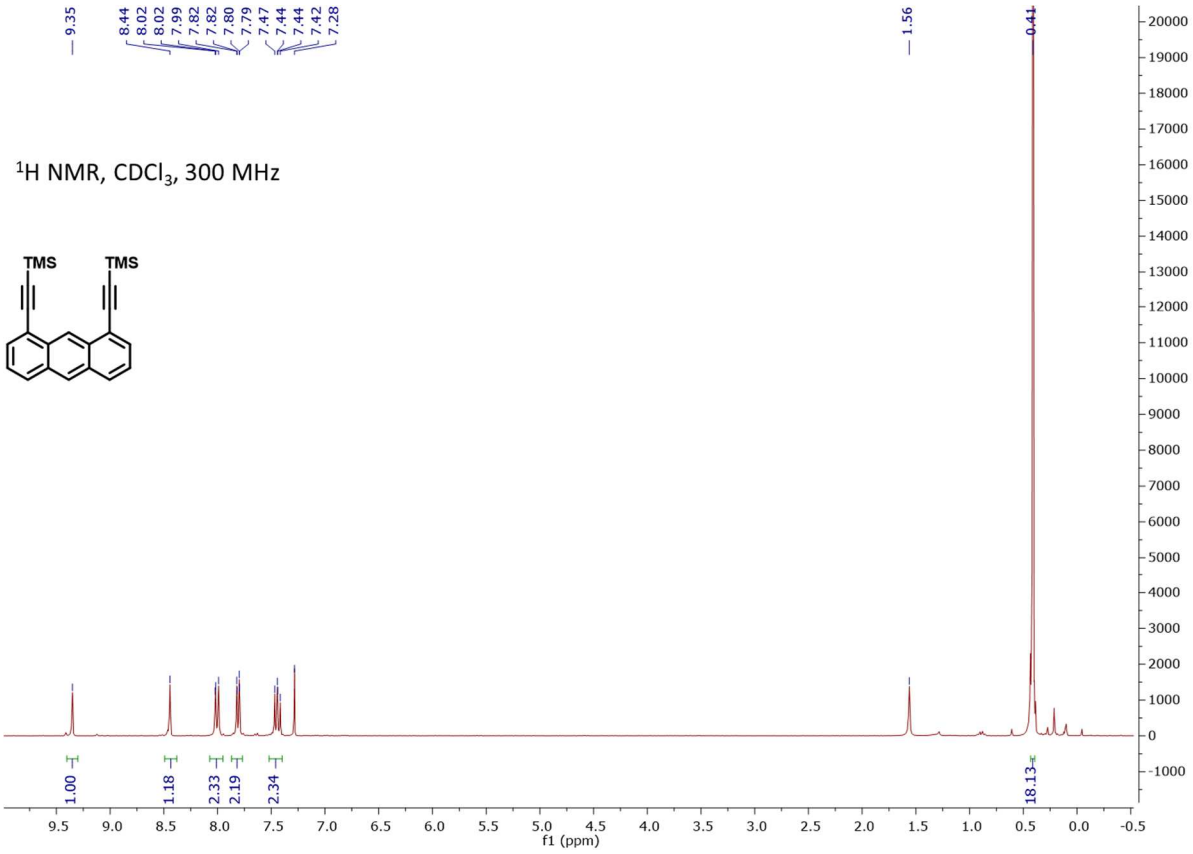

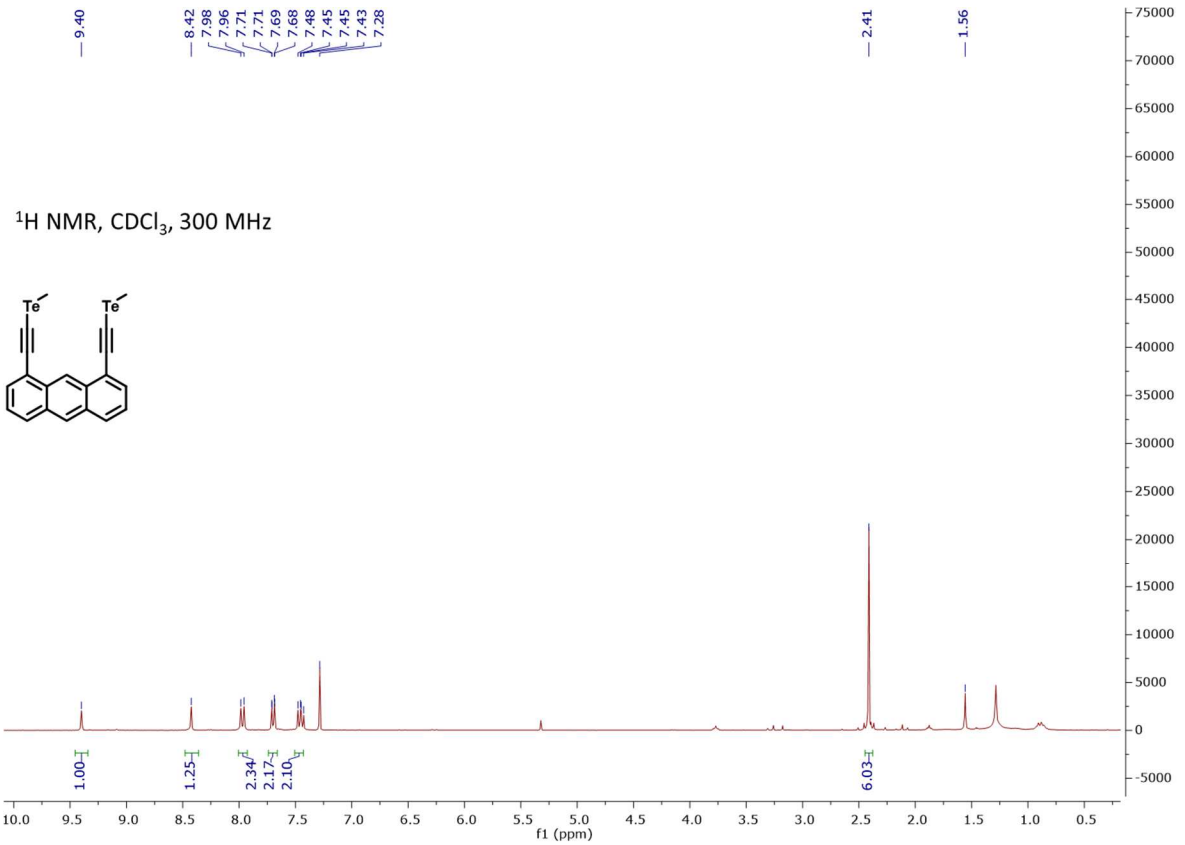

^{1}H NMR, $CDCl_3$, 300 MHz

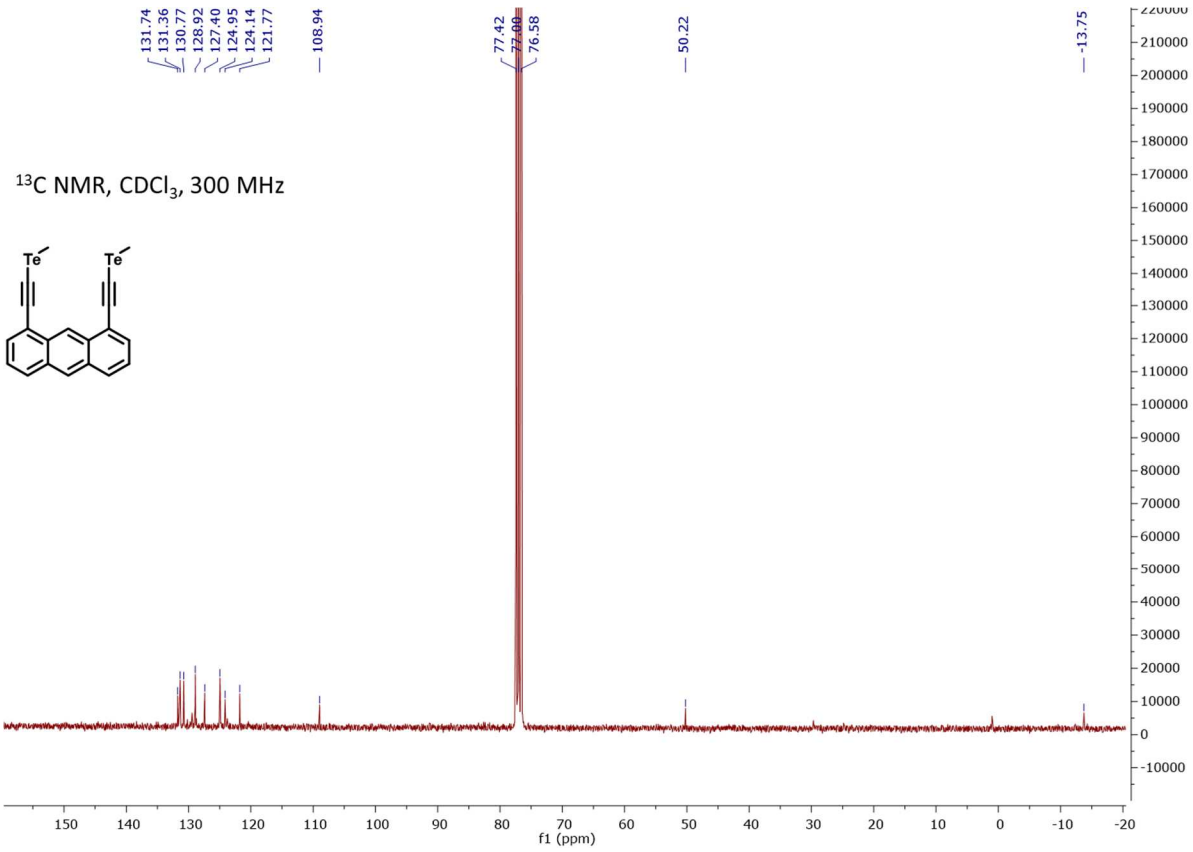

^{13}C NMR, $CDCl_3$, 300 MHz

B. Co-Crystallization experiments:

BTMEA•bpe : To a solution of DTMEA (10 mg) in EtOAc (0.5 ml) was layered with 4,4'-bipyridine (3.6 mg, 1 equiv.) dissolved in EtOAc (0.5 ml). Slow evaporation of solvent resulted in the formation of red prism shaped crystals. Mp: 137-138 ^{o}C; Anal. Calcd for $C_{32}H_{26}N_2Te_2$: C, 55.40; H, 3.78; N, 4.04 found: C, 56.27; H, 3.90; N, 4.43.

BTMEA•bpy-pip : To a solution of DTMEA (10 mg) in EtOAc (0.5 ml) was layered with (bipy-pip) bispyridine-piperazine (4.7 mg, 1 equiv.) dissolved in EtOAc (0.5 ml). Slow evaporation of solvent resulted in the formation of red shaped crystals. Mp: 193-194 ^{o}C; Anal. Calcd for $C_{34}H_{30}N_4Te_2$: C, 54.56; H, 4.03; N, 7.47 found: C, 54.24; H, 3.79; N, 7.07.

BTMEA•azopy : To a solution of DTMEA (10 mg) in EtOAc (0.5 ml) was layered with azobipy (3.6 mg, 1 equiv.) dissolved in EtOAc (0.5 ml). Slow evaporation of solvent resulted in the formation of red plate shaped crystals. Mp: 122-124 ^{o}C; crystals were obtained together with starting compounds, hindering the isolation of a bulk sample for elemental analysis.

BTMEA•(bpen)$_2$: To a solution of DTMEA (10 mg) in EtOAc (0.5 ml) was layered with bpen (3.6 mg, 1 equiv.) dissolved in EtOAc (0.5 ml). Slow evaporation of solvent resulted in the formation of orange prism shaped crystals. Mp: 138-139 ^{o}C; crystals were obtained together with starting compounds, hindering the isolation of a bulk sample for elemental analysis.

C. Crystallography Details about data collection and solution refinement are given in Table S1. Data collections were performed at RT on an APEXII Bruker-AXS diffractometer equipped with a CCD camera for all compounds. Structures were solved by direct methods using the *SIR97* program[5] or by dual-space algorithm using SHELXT[6] and then refined with full-matrix least-square methods based on F^2 (*SHELXL-2014*)[7] with the aid of the *WINGX* program.[8] All non-hydrogen atoms were refined with anisotropic atomic displacement parameters. H atoms were finally included in their calculated positions. Crystallography data (in cif format) have been deposited with CCDC with deposition numbers CCDC-2059424-2059427.

Table S1 Crystallographic data

Compound	**BTMEA•bpe**	**BTMEA•bpy-pip**	**BTMEA•azopy**	**BTMEA•(bpen)$_2$**
CCDC	2059424	2059425	2059426	2059427
Formulae	$C_{32}H_{26}N_2Te_2$	$C_{34}H_{30}N_4Te_2$	$C_{30}H_{22}N_4Te_2$	$C_{44}H_{34}N_4Te_2$
FW (g.mol^{-1})	693.75	749.82	693.71	873.95
System	monoclinic	monoclinic	monoclinic	triclinic
Space group	$P2_1/n$	$P2_1/n$	$P2_1/n$	$P\bar{1}$
a (Å)	10.6599(7)	18.3874(6)	10.8282(19)	10.390(2)
b (Å)	24.9103(15)	10.4516(3)	24.258(4)	11.252(2)
c (Å)	11.7016(8)	32.5186(10)	11.763(2)	16.357(4)
α (deg)	90	90	90	98.128(7)
β (deg)	113.683(2)	104.148(2)	115.480(6)	91.282(7)
γ (deg)	90	90	90	96.440(7)
V (Å^3)	2845.6(3)	6059.8(3)	2789.3(8)	1879.7(7)
T (K)	296(2)	296(2)	294(2)	300(2)
Z	4	8	4	2
Cryst. dim. (mm)	0.23×0.18×0.12	0.27×0.04×0.03	0.28×0.24×0.03	0.12×0.05×0.02
D_{calc} (g.cm^{-1})	1.619	1.644	1.652	1.544
μ (mm^{-1})	2.072	1.955	2.116	1.588
Total refls	21215	43376	34265	44808
Abs. corr.	multi scan	multi scan	multi scan	multi scan
T_{min}, T_{max}	0.646, 0.780	0.910, 0.943	0.558, 0.938	0.909, 0.969
Uniq refls (R_{int})	6490 (0.0357)	13910 (0.0484)	6342 (0.0499)	8660 (0.0779)
Uniq refls (I > 2σ(I))	4174	7718	4997	5529
R_1, wR_2 (I > 2σ(I))	0.0501, 0.1025	0.0576, 0.1163	0.0776, 0.1612	0.0463, 0.1113
R_1, wR_2 (all data)	0.0912, 0.118	0.1225, 0.1393	0.099, 0.1725	0.0867, 0.1355
GOF	1.023	1.018	1.24	1.019
Res. dens. (e$^-$/Å^3)	0.988, −0.579	1.103, −0.792	1.051, −0.945	1.451, −0.601

D. Theoretical calculations

Molecular structures of **BTMEA** and the four ChB acceptors (bipy-pip, bpe, azopy and bpen) have been optimized in gas phase (vacuum) with Gaussian09 software[9] using Density Functional Theory. B3LYP functional was used, completed with D3 dispersion Grimme dispersion correction.[10] The Def2TZVPP basis set was employed for all atoms, including a pseudo-potential for the heaviest Te atom taken from the EMSL library.[11] Frequency calculations were performed in order to check that true energy minima were obtained. Isosurfaces of electron density (ρ = 0.002 a.u.) mapped with the corresponding total electrostatic potential were calculated and drawn with AIMAll software.[12]

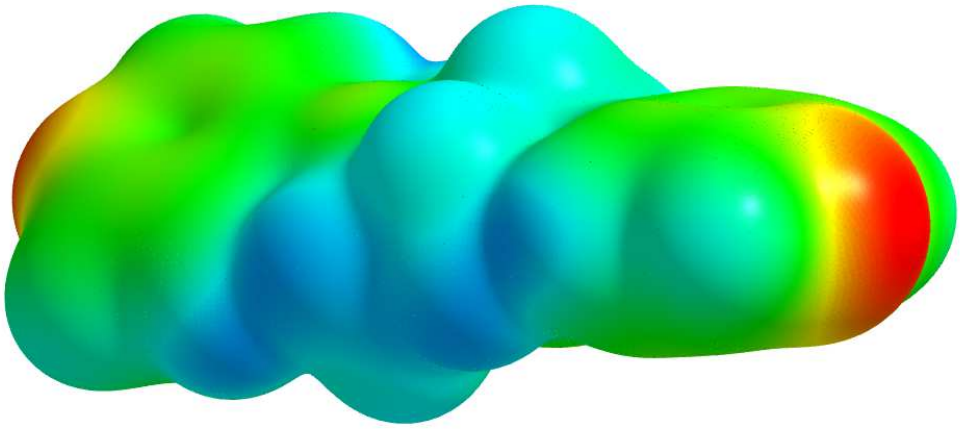

Fig. S1 ESP (-0.07 a.u. :red to +0.07 a.u.: blue) on 0.002 a.u. isodensity surface of bpy-pip

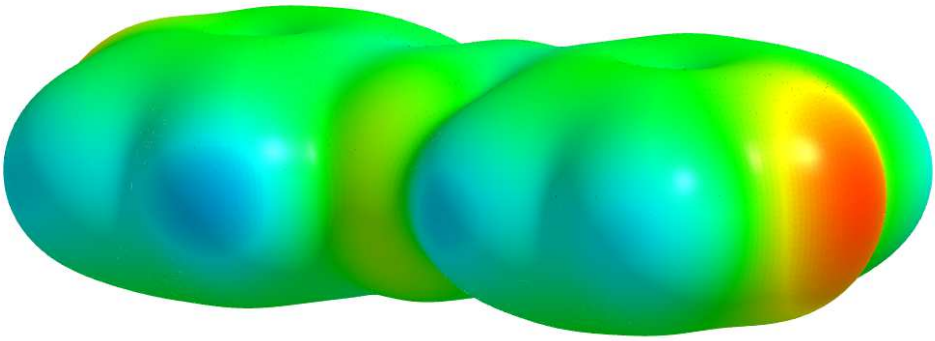

Fig. S2 ESP (-0.07 a.u. :red to +0.07 a.u.: blue) on 0.002 a.u. isodensity surface of azopy

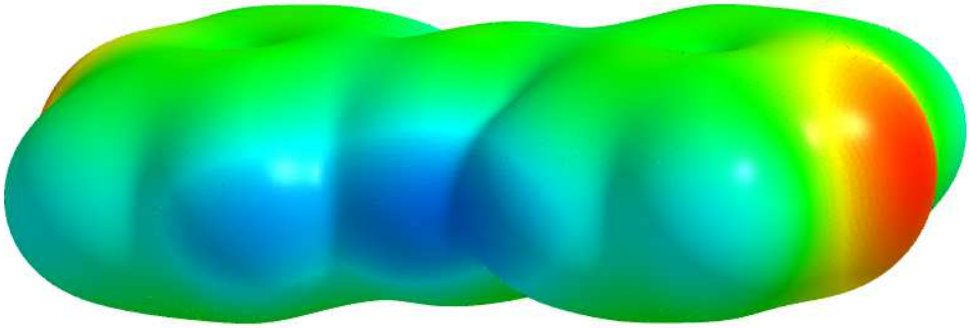

Fig. S3 ESP (-0.07 a.u. :red to +0.07 a.u.: blue) on 0.002 a.u. isodensity surface of bpen

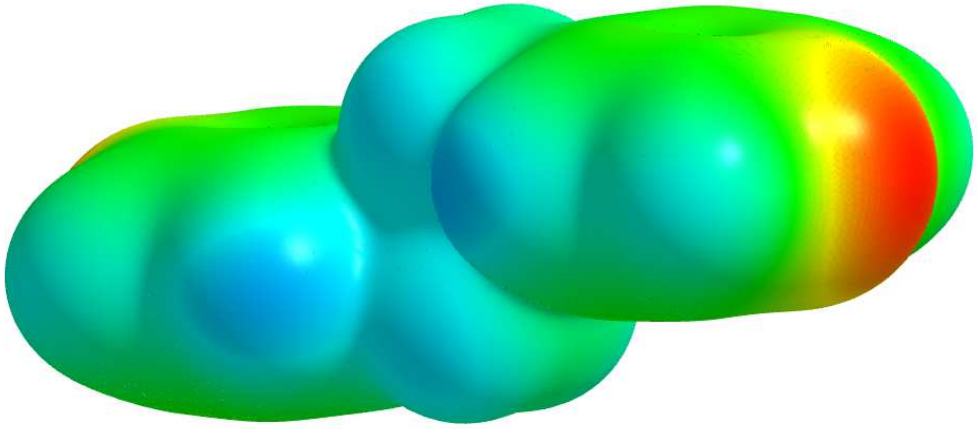

Fig. S4 ESP (-0.07 a.u. :red to +0.07 a.u.: blue) on 0.002 a.u. isodensity surface of bpe

E. Analyses of the ChB interactions between rectangles

Besides the short and highly directional (C≡C)−Te•••N ChB interactions leading to the formation of the supramolecular rectangles, other, probably weaker ChB interactions involving the second σ-hole on the tellurium atoms in **BTMEA** in the prolongation of the Me−Te bonds, have been identified in **BTMEA•bpy-pip**. As shown in Figure S6, one nitrogen (N2) of the piperidine central ring of bpy-pip acts as a ChB acceptor toward the second σ-hole on the Te(3) atom, with a Te•••N distance at 3. 861(6) Å, to be compared to the van der Waals contact distance of 3.61 Å. Albeit slightly longer (See in that respect the revised vdW radii reported by Chernyshov *et al*.),[15] its directionality is a clear indication of a secondary ChB interaction.

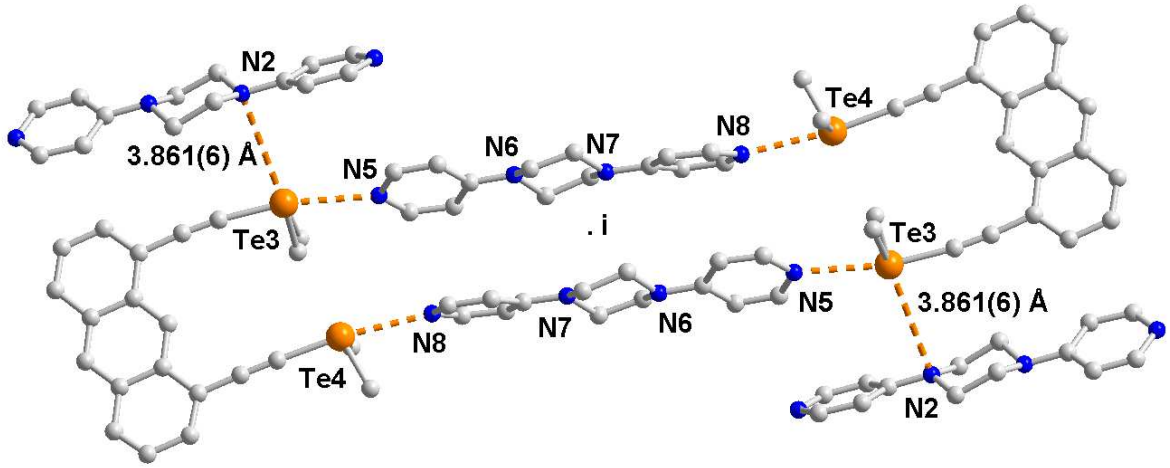

Figure S5. Detail of the surrounding of one of the two crystallographic independent rectangles in **BTMEA•bpy-pip**.

F. References

1) F. Louerat, P. C. Gros and Y. Fort, *Synlett* 2006, 1379-1383
2) A. Borissov, I. Marques, J. Y. C. Lim, V. Félix, M. D. Smith and P. D. Beer, *J. Am. Chem. Soc.*, 2019, **141**, 4119–4129.
3) M. Perez-Trujillo, I. Maestre, C. Jaime, A. Alvarez-Larena, J. F. Piniella and A. Virgili, *Tetrahedron: Asymmetry*, 2005, **16**, 3084–3093.
4) T. K. Wijethunga, M. Đakovic, J. Desper and C. B. Aakeroy, *Acta Cryst. B*, 2017, **73**, 163–167.
5) A. Altomare, M. C. Burla, M. Camalli, G. Cascarano, C. Giacovazzo, A. Guagliardi, A. G. G. Moliterni, G. Polidori and R. Spagna, *J. Appl. Cryst*., 1999, **32**, 115–119.
6) G. M. Sheldrick, *Acta Cryst*. 2015, **A71**, 3−8
7) G. M. Sheldrick, *Acta Cryst*. 2015, **C71**, 3−8.
8) L. J. Farrugia, *J. Appl. Cryst*., 2012, **45**, 849–854.
9) M. J. Frisch, G. W. Trucks, H. B. Schlegel, G. E. Scuseria, M. A. Robb, J. R. Cheeseman, G. Scalmani, V. Barone, B. Mennucci, G. A. Petersson, H. Nakatsuji, M. Caricato, X. Li, H. P. Hratchian, A. F. Izmaylov, J. Bloino, G. Zheng, J. L. Sonnenberg, M. Hada, M. Ehara, K. Toyota, R. Fukuda, J. Hasegawa, M. Ishida, T. Nakajima, Y. Honda, O. Kitao, H. Nakai, T. Vreven, J. A. Montgomery, Jr., J. E. Peralta, F. Ogliaro, M. Bearpark, J. J. Heyd, E. Brothers, K. N. Kudin, V. N. Staroverov, R. Kobayashi, J. Normand, K. Raghavachari, A. Rendell, J. C. Burant, S. S. Iyengar, J. Tomasi, M. Cossi, N. Rega, J. M. Millam, M. Klene, J. E. Knox, J. B. Cross, V. Bakken, C.

Adamo, J. Jaramillo, R. Gomperts, R. E. Stratmann, O. Yazyev, A. J. Austin, R. Cammi, C. Pomelli, J. W. Ochterski, R. L. Martin, K. Morokuma, V. G. Zakrzewski, G. A. Voth, P. Salvador, J. J. Dannenberg, S. Dapprich, A. D. Daniels, Ö. Farkas, J. B. Foresman, J. V. Ortiz, J. Cioslowski, and D. J. Fox, Gaussian 09 (Gaussian, Inc., Wallingford CT, 2009).

10) S. Grimme, J. Antony, S. Ehrlich and H. Krieg, *J. Chem. Phys*., 2010, **132**, 154104.
11) B. P. Pritchard, D. Altarawy, B. Didier, T. D. Gibson and T. L. Windus. *J. Chem. Inf. Model*. 2019, **59**(11), 4814-4820.
12) AIMAll (Version 19.10.12), T. A. Keith, TK Gristmill Software, Overland Park KS, USA, 2019 (aim.tkgristmill.com).
13) M. Fourmigué and A. Dhaka, *Coord. Chem. Rev*., 2020, **403**, 213084
14) Y. V. Torubaev, D. K. Rai, I. V. Skabitsky, S. Pakhira and A. Dmitrienko, *New J. Chem*., 2019, **43**, 7941−7949.
15) I.Y. Chernyshov, I.V. Ananyev and E. A. Pidko, *ChemPhysChem*, 2020, **21**, 370−376.